

# High Gain Wideband Filtering Quasi-Yagi Antenna Based on High-Order Mode of SSPPs

Daotong Li, *Senior Member, IEEE*, Ning Pan, Hao Wang, Jiang Dong, Qi Jiang, Ying Liu, Naoki Shinohara, *Fellow, IEEE*, and Qiang Chen, *Senior Member, IEEE*

**Abstract**—A high-gain wideband filtering antenna based on the high-order mode of spoof surface plasmon polaritons (SSPPs) is proposed. Excellent filtering characteristics with six radiation nulls are obtained from the first high-order mode (mode 1) of SSPPs feedline. A novel Ground-Free Single-Unit Transition Structure (GFSTS) is introduced to facilitate smooth momentum transition and impedance matching between the SSPPs feedline and driven dipole. The inherent bandpass response of the high-order mode of SSPPs enables the proposed filtering antenna to operate without additional filtering structures, thus avoiding insertion loss and achieving a simplified design. The low-loss transmission characteristic of the SSPPs feedline, along with the elimination of insertion loss from external filtering components, enhances the radiation efficiency of the quasi-Yagi antenna. To validate the feasibility of proposed antenna, a prototype is fabricated and measured. Good end-fire characteristics are obtained with bandwidth of 3.76 to 6.3 GHz (50.5%), peak gain of 9.98 dBi and the out-of-band suppression larger than 18.8 dB. The measured results are in good agreement with the simulation.

**Index Terms**—filtering antenna, spoof surface plasmon polaritons (SSPPs), high-order mode, quasi-Yagi antenna

## I. INTRODUCTION

WITH the rapid advancement of wireless communication technologies, antennas—being a crucial component of communication systems—are evolving toward greater integration and multifunctionality. Filtering antennas can effectively suppress interference signals and reduce mutual coupling between antenna elements operating at different frequencies, thereby enabling the design of more compact systems. The filtering quasi-Yagi antenna has been widely studied due to its low profile, low cost, end-fire radiation pattern and high directivity[1], [2], [3].

This work was supported in part by the Chongqing Natural Science Foundation under Grants: CSTB2024NSCQ-MSX1038, CSTB2024NSCQ-MSX1217, in part by the National Natural Science Foundation of China under Grant 61801059, and in part by the Function development project for large and valuable instruments under Grant gnkf2023009.

Daotong Li, Ning Pan, Hao Wang, Jiang Dong, Qi Jiang, and Ying Liu are with School of Microelectronics and Communication Engineering, Chongqing University, Chongqing 400044, China (e-mail: dli@cqu.edu.cn).

Daotong Li and Naoki Shinohara are with the Research Institute for Sustainable Humanosphere, Kyoto University, Kyoto 606-8501, Japan.

Qiang Chen is with the Department of Communications Engineering, Tohoku University, Sendai 980-8579, Japan (e-mail: qiang.chen.a5@tohoku.ac.jp).

Color versions of one or more of the figures in this article are available online at <http://ieeexplore.ieee.org>.

Filtering antennas can be broadly classified into three categories based on design approaches. The first method involves integrating a filter into the antenna's feeding network, either by adding a complete filter[1], [4] or specific structures[5], [6], [7] to generate transmission zeros for filtering functionality. This approach allows independent antenna and filter design but leads to low integration and high insertion loss, reducing radiation efficiency. An alternative approach modifies the radiator to suppress or cancel the radiating currents, thereby creating radiation nulls on either side of the passband using techniques such as parasitic elements[8], slots[9], [10], or shorting pins[11], [12]. These antennas achieve higher integration levels, with radiation nulls minimally affecting operational band performance. However, their complex structures make design optimization challenging. Additionally, certain design schemes only generate radiation nulls in specific directions[10], [12], while non-negligible gain remains in other directions, resulting in insufficient interference rejection. Lastly, filter synthesis integrates the radiator as the filter's final resonator, enabling radiating capabilities[13], [14], [15]. Antennas designed with this approach excel in integration, bandwidth, and selectivity. However, the insertion loss of the filter is inevitable, thereby reducing the overall radiation efficiency. In summary, most reported filtering antennas feature a broadside radiation pattern, with their filtering capabilities often accompanied by transmission losses that reduce gain. Reducing these losses introduced is a crucial approach to improving the gain of filtering antennas.

SSPPs are sub-wavelength periodic structures that support electromagnetic wave modes analogous to Surface Plasmon Polaritons at lower frequencies. SSPPs offer high field confinement, low loss, and conformability, making them ideal for recent microwave applications like power dividers[16], filters[17], [18], and antennas[19], [20].

The single-mode transmission characteristics of the high-order mode in SSPPs can be achieved using a simple and compact transition structure, facilitating the design of various BPFs with excellent in-band transmission performance[21], [22]. In addition, exciting multiple order modes of SSPPs can generate multiple passbands and eliminating the stopbands between these passbands to achieve broadband performance is feasible. For example, in [23], a multi-band antenna is realized by designing units that support multiple high-order modes of SSPPs. The subsequent introduction of I-shaped resonators eliminated the stopbands between the individual passbands,

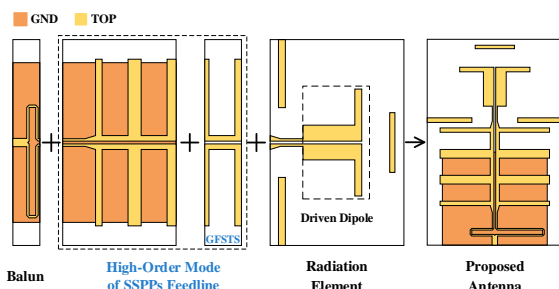


Fig. 1. Structural diagram of the proposed filtering antenna.

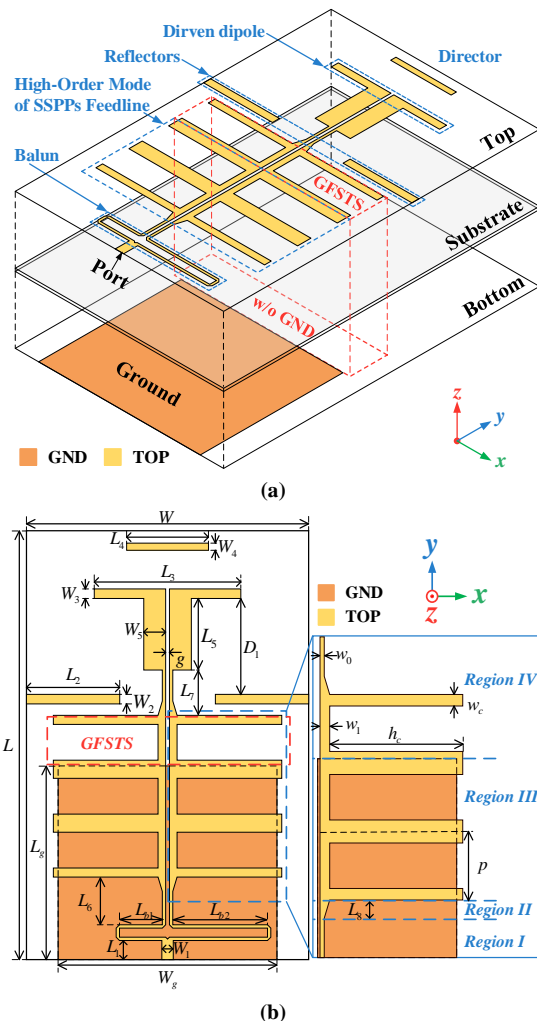
resulting in an ultra-wideband end-fire antenna. Based on the fundamental mode of SSPPs, some filtering antennas[20], [24]and end-fire antennas[19], [25] have been reported. antennas[20], [24]and end-fire antennas[19], [25] have been reported. The filtering performance in these designs is mainly achieved through via holes and ring resonators[24] or by utilizing the low-pass characteristics of the fundamental mode of SSPPs in combination with other techniques[20]. The introduction of SSPPs is primarily aimed at reducing transmission loss to enhance gain. However, existing filtering antennas that incorporate SSPPs technology still rely on additional filtering structures to achieve their filtering functionality. As a result, these antennas suffer from non-negligible losses and exhibit relatively complex structures as well as enormous sizes. To the best of the authors' knowledge, filtering antennas solely relying on SSPPs have not yet been reported.

In this paper, a high gain wideband filtering quasi-Yagi antenna is implemented relying on the single-mode transmission and low-loss characteristics of SSPPs. The feedline supporting the high-order mode of SSPPs not only provides filtering characteristics independently, avoiding additional lossy filtering structures, but also enhances the antenna gain due to SSPPs' inherent low-loss properties. The proposed novel Ground-Free Single-Unit Transition Structure (GFSTS), achieving significant size reduction compared to traditional tapered transitions, facilitates smooth momentum transition between the high-order mode of SSPPs and the driven dipole. The SSPPs feedline and balun generate six radiation nulls (RN), endowing the antenna with excellent frequency selectivity and strong stopband suppression. A prototype of proposed antenna achieves a wide -10dB impedance bandwidth from 3.76 to 6.3 GHz and a peak gain of 9.98 dBi.

The arrangement of this paper is as follows. Section II is the configuration of the proposed antenna. Section III is the mechanism of metallic strips feedline supporting high-order mode of SSPPs of the proposed high gain wideband filtering quasi-Yagi antenna. Section IV gives the fabrication and experimental results of the proposed high gain wideband filtering quasi-Yagi antenna based on high-order mode of SSPPs. Finally, conclusion is drawn in Section V.

## II. ANTENNA CONFIGURATION

As shown in Fig. 1, the overall structure of the antenna consists of four main components: the balun, high-order mode



dispersion curve is illustrated in Fig. 3. The top and bottom layers of the Rogers 5880 substrate are patterned with U-shaped metallic strips and a ground plane, respectively. The thickness of the dielectric substrate is 0.787 mm. To minimize the influence of material thickness on the simulation results, the thickness of the metallic layers is set to 0.035 mm. In order to excite the high-order mode of SSPPs of the U-shape unit, the depth of the groove  $h_c$  of the unit must be greater than the period  $p$ . The number of modes  $N$  for the SSPPs can be approximately expressed as:

$$N = 1 + \text{int}(h_c / p) \quad (1)$$

Numerical analysis of the unit's dispersion characteristics is performed using the eigenmode solver in CST Microwave Studio. In Fig. 3, the dispersion curves exhibit multiple branches across different frequency bands, demonstrating typical SPP-like behavior. As the frequency increases, both curves diverge from the light line in free space, entering the slow-wave region, and reach a horizontal asymptotic frequency limit at the edge of the first Brillouin zone. This result indicates that the designed U-shape unit simultaneously supports both fundamental (mode 0) and high-order (mode 1) modes of SSPPs, which is consistent with the number of modes obtained from (1). These modes correspond to distinct frequency bands that are isolated from each other, allowing for the formation of a passband for single-mode transmission only.

As mentioned above, mode 1, which is isolated from mode 0, exhibits bandpass response characteristics. Therefore, no additional filtering structures are required, and the desired passband can be achieved by simply designing the geometry of the SSPPs unit, as shown in Fig. 4. A simple and compact trapezoidal structure enables smooth matching between the SSPPs waveguide operating in mode 1 and the microstrip line, as shown in region II of Fig. 2. However, since it cannot provide smooth matching for the SSPPs waveguide operating in mode 0, this transition structure effectively suppresses low-frequency signals from passing through the passband associated with mode 0, thereby enhancing the out-of-band rejection of the filtering antenna. Simulation results show that the in-band insertion loss is less than 0.5 dB, and the return loss is better than 10 dB. To further verify the proposed antenna's support for the high-order mode of SSPPs, the simulated electric field distribution of the proposed antenna at 5.8 GHz is illustrated in Fig. 5(b). As can be observed, the energy is efficiently transmitted to the driven dipole, and the feeding line supporting SSPPs shows an electric field distribution consistent with that of the U-shape unit in the mode 1 region, as shown in Fig. 5(a) and obtained from the eigenmode simulation. The proposed antenna exhibits similar typical electric field characteristics. The electromagnetic energy is tightly confined near the metallic strips, with the maximum of electric field magnitude symmetrically distributed along the geometric axis of the unit. Moreover, each metallic strip of the U-shaped unit can be divided into two distinct regions based on the direction of the  $z$ -component electric field distribution on its surface. From the side view in Fig. 5(c), a strong confinement effect is evident, demonstrating the characteristic binding of the field near the structure.

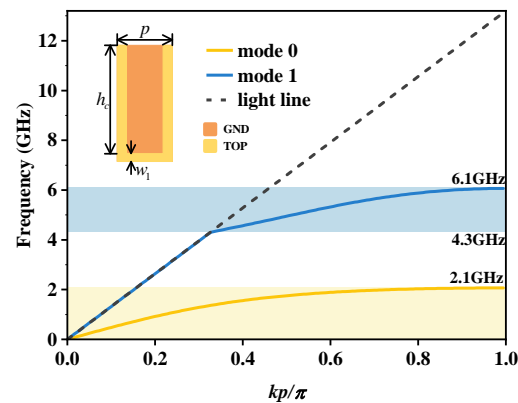


Fig. 3. Simulated dispersion curves for the first two modes of the U-shape unit in Fig. 2 ( $h_c=22\text{mm}$ ,  $p=11.3\text{mm}$ ,  $w_c=1.9\text{mm}$ , and  $w_l=1.6\text{mm}$ ).

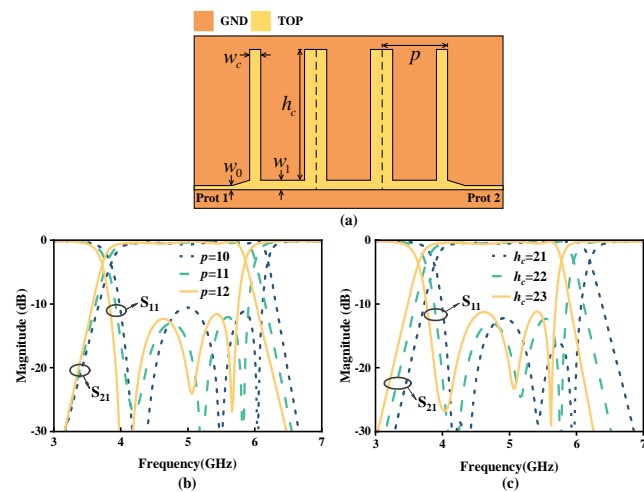


Fig. 4. (a) Configurations of bandpass filter based on mode 1 of proposed U-shape unit and its simulated S-parameters against (b) parameter  $p$  and (c) parameter  $h_c$ .

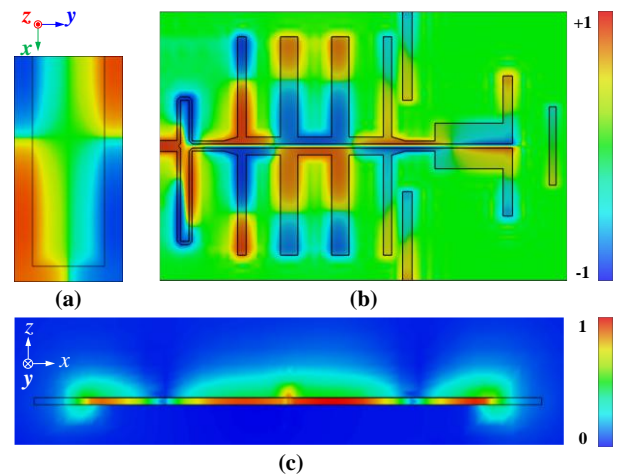


Fig. 5. Normalized  $z$  component of the electric field distributions of (a) mode 1 at asymptotic frequencies 6.1GHz and (b) the proposed filtering antenna at the frequencies of 5.8GHz. (c) Normalized amplitude of electric field in the cross-section perpendicular to the strip. The color bar indicates the electric field polarity and field strength in logarithm.

### B. Principle of Ground-Free Single-Unit Transition Structure

As previously mentioned, the energy is tightly confined

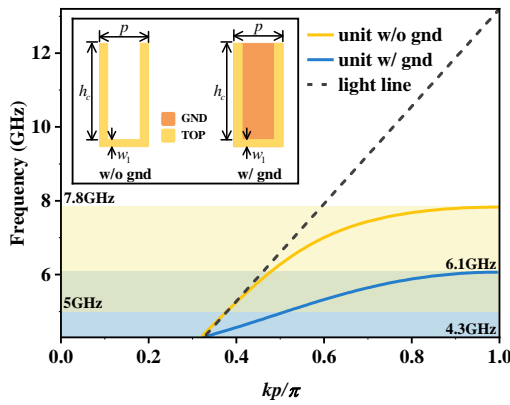


Fig. 6. The dispersion curves for mode 1 of the grounded U-shaped unit and the ground-free U-shaped unit.

around the metallic strips, allowing only signals within the passband corresponding to mode 1 to propagate. However, it is challenging to directly feed energy from the SSPPs strips into the driven dipole. To address this issue, the novel GFSTS is proposed, enabling seamless momentum transition and impedance matching between the high-order mode of SSPPs filtering structure and the driven dipole.

The dispersion curves for mode 1 of the grounded U-shaped unit and the ground-free U-shaped unit are shown in Fig. 6. The cutoff frequency of the ground-free U-shaped unit is higher than that of the grounded U-shaped unit, indicating relatively weaker electromagnetic confinement in the ground-free unit. Additionally, the propagation wavenumber in the y-direction for the ground-free U-shaped unit falls between that of the grounded U-shaped unit and the light line. The GFSTS, employing a ground-free U-shaped unit to bridge the SSPPs feedline and the driven dipole, facilitates a smooth momentum transition. This structure enables the propagating SPP waves to be effectively converted into guided waves, in contrast to a direct transition to the driven dipole. As a result, energy is efficiently fed into the driven dipole while maintaining the filtering characteristics of the high-order mode of SSPPs.

However, to achieve broadband filtering characteristics, ensure efficient transition from the SSPPs structure to the driven dipole, and maintain compact antenna dimensions, the proposed novel transition structure is designed with a single ground-free U-shaped unit. Fig. 7 illustrates the relationship between the number of ground-free U-shaped units in the transition structure and the antenna performance. Compared to the reference antenna, the antenna with a single-unit transition structure shows superior performance in terms of realized gain in the end-fire direction (+y axis), return loss, and out-of-band suppression, confirming the necessity of the single-unit design.

### C. High-Gain Characteristics of the Antenna

The quasi-Yagi antenna design has been employed to achieve end-fire radiation. The integration of the high-order mode of SSPPs with the quasi-Yagi antenna ultimately achieves high gain and broadband characteristics. As shown in the gain comparison curve in Fig. 8, the reflector, director, and ground reflection effectively enhance the antenna's aperture,

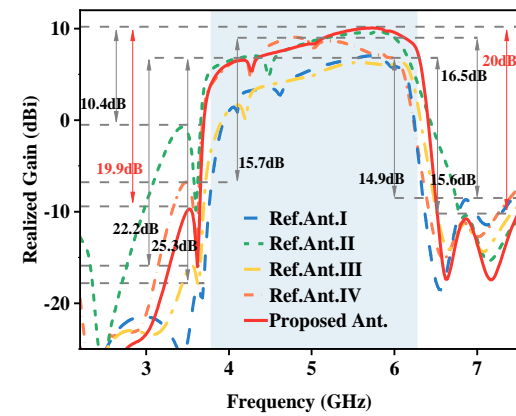
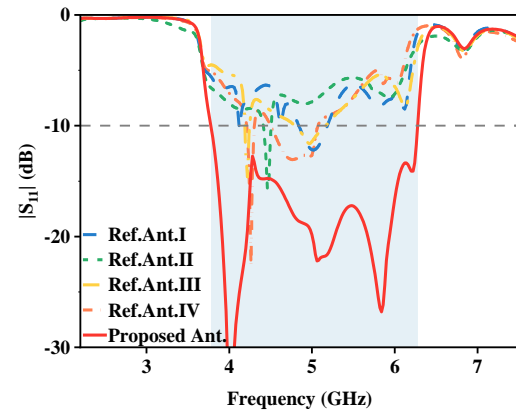
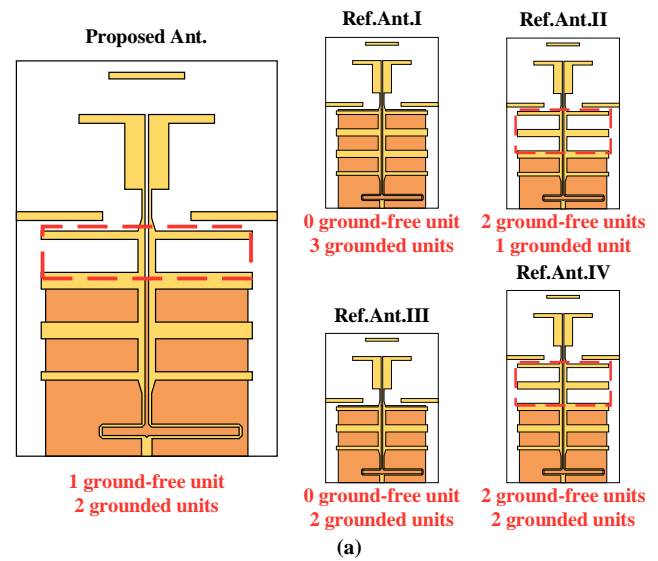


Fig. 7. (a) Configurations of the reference and proposed antennas and their corresponding performance: (b)  $|S_{11}|$  and (c) realized gain.

resulting in a significant gain improvement compared to a standard dipole antenna. Additionally, the configuration of the reflector and its relative position to the SSPPs provides excellent directivity for the antenna.

The feed line supporting the high-order mode of SSPPs exhibits relatively lower transmission loss, which improves the antenna's radiation efficiency and enhances its gain. According

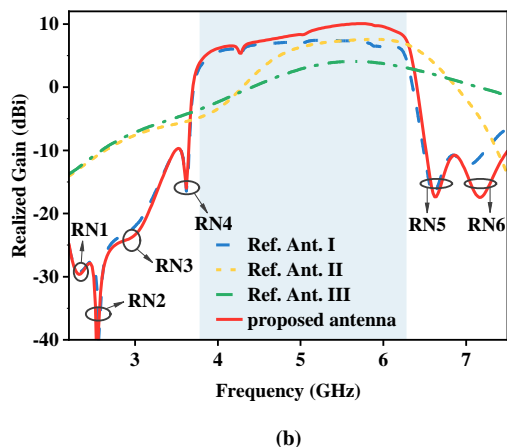
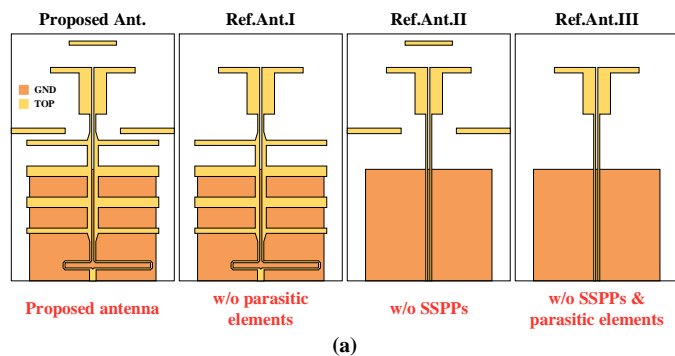


Fig. 8. (a) Configuration and (b) simulated results of realized gain with/without SSPPs structure, reflectors, and director.

to perturbation theory, the attenuation constant of a microwave transmission line can be expressed as:

$$\alpha \approx \frac{\omega_0 \varepsilon \tan \delta \iint_{\Delta S} |\vec{E}_0|^2 dS}{\iint_S (\vec{E}_0^* \times \vec{H}_0 + \vec{H}_0^* \times \vec{E}_0) \cdot dS} \quad (2)$$

where  $\Delta S$  and  $S$  represent the areas of the substrate and total space, respectively, and the denominator represents twice the mean power flow of the transmission line. It can be observed that for transmission lines with equal power transmission, the attenuation constant  $\alpha$  is positively correlated with the distribution of electric field energy within the substrate. From the electric field distribution characteristics in Fig. 5(c), compared to traditional structures, such as microstrip lines, there are more electromagnetic fields confined to the air around SSPPs, while the electromagnetic fields distributed in the dielectric substrate are correspondingly weaker. Therefore, according to (2), the SSPPs feedline employed in the proposed antenna exhibits lower transmission loss.

Therefore, due to the unique electric field distribution characteristics of the SSPPs structure, the SSPPs feedline used in this work exhibits inherently lower loss, enabling higher transmission efficiency. Additionally, the single-mode transmission characteristics of the high-order mode of SSPPs can independently achieve the antenna's filtering function without requiring additional filtering structures, which may otherwise reduce radiation efficiency. This approach further

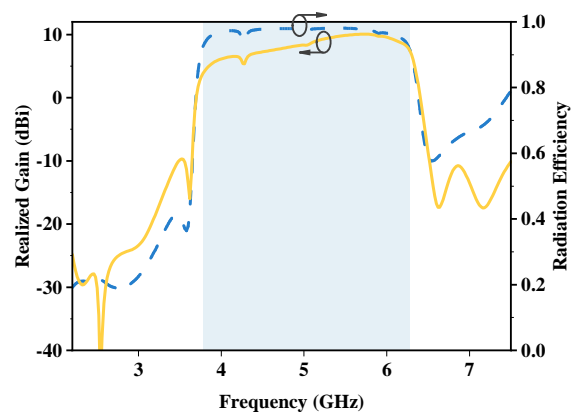


Fig. 9. Simulated result of realized gain and radiation efficiency of proposed filtering antenna.

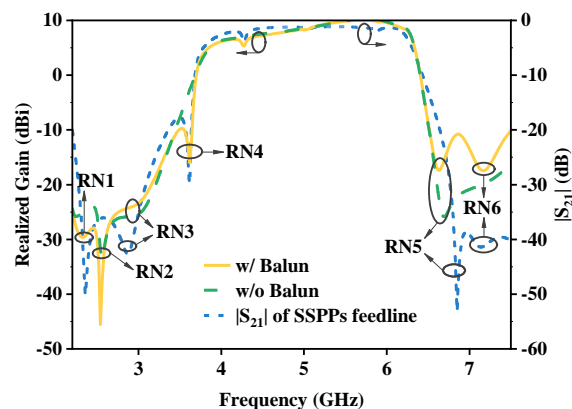


Fig. 10. Simulated result of realized gain with/without balun and  $|S_{21}|$  of SSPPs feeding line.

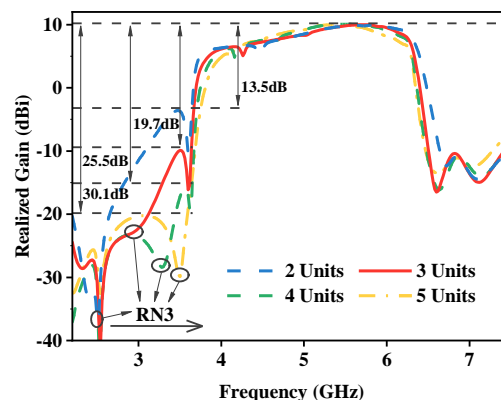


Fig. 11. Simulated result of realized gain of proposed antenna with different total number of U-shape units.

enhances the overall radiation efficiency. Through comparative simulations, the gain curve shown in Fig. 9 demonstrates that the antenna achieves not only filtering characteristics but also a significant gain enhancement, with a simulated peak gain reaching 10.1 dBi and the simulated in-band radiation efficiency over 94%.

#### D. Mechanism of the Radiation Nulls

As shown in Fig. 8, RN1 to RN6 are introduced in the

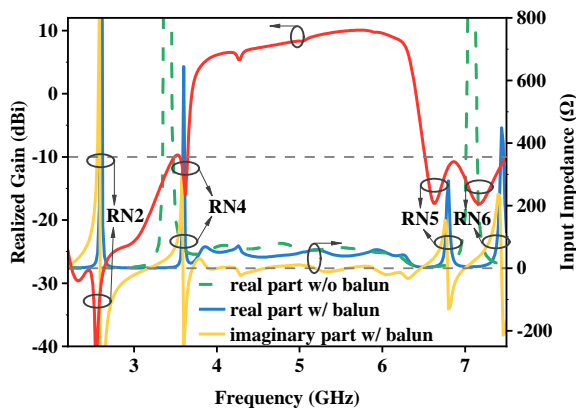


Fig. 12. Realized gain of the proposed antenna and input impedance with/without balun.

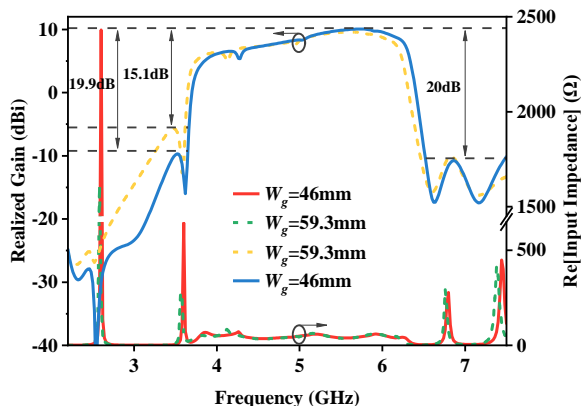


Fig. 13. Realized gain and real part of input impedance of the proposed antenna against parameter  $W_g$ .

stopbands by the proposed antenna. The following analysis will investigate the mechanisms behind the generation of these radiation nulls. The antenna feed line operates in the high-order mode of SSPPs, introducing natural stopbands that arise from the interactions between different modes of the SSPPs. This results in the formation of three radiation nulls located at 2.32, 2.54 and 6.64 GHz, respectively, namely RN1, RN2 and RN5, corresponding to the transmission coefficient curve of the SSPP feed structure in Fig. 10. The depression in the radiation pattern of the proposed antenna at 2.96 GHz in the end-fire direction has led to the formation of a spatial radiation null, labeled as RN3. It is noteworthy that within a certain range, the more units the SSPPs feedline consists of, the better the roll-off of the stopband will be. As shown in Fig. 11, with the increase in the number of units, RN3 shifts toward higher frequencies, thereby improving the frequency selectivity of the antenna. To balance the antenna's performance and profile, the proposed high gain filtering quasi-Yagi antenna employs a design with three units. Additionally, the new resonance modes generated by the metallic strips broaden the bandwidth of the proposed antenna.

To facilitate feeding, a balun is designed as shown in Fig. 2(b) to excite the dipole for radiating electromagnetic waves. As shown in Fig. 12, after the introduction of the balun, the real part of the antenna's input impedance significantly increases at 3.6 GHz and 7.4 GHz, preventing efficient energy transfer to

the radiating elements and thus generating radiation nulls RN4 and RN6, which improves the roll-off of the stopband of the proposed antenna. The introduction of the balun causes the proposed antenna to further severely mismatch at RN2, increasing the depth of RN2. Additionally, the impedance peak at 7.1 GHz shifts slightly toward the lower frequencies and decreases, which reduces the depth of RN5, as illustrated in Fig. 10. However, a minor peak appears at 4.2 GHz on the real part of the input impedance curve, causing a slight suppression in antenna gain. The use of the balun not only simplifies testing but also improves the roll-off rate of the lower stopband, enhancing the antenna's frequency selectivity.

Additionally, reducing the ground width  $W_g$ , as shown in Fig. 2(b), increases the real part of the input impedance of the proposed antenna from  $1500 \Omega$  to  $2500 \Omega$ , which improves the depth of RN2 from  $-26$  dBi to  $-45$  dBi, thereby effectively enhancing the suppression of the lower stopband, as shown in Fig. 13.

#### IV. FABRICATION AND MEASUREMENT RESULTS

To verify the feasibility of the design, a prototype of the proposed High Gain Wideband Filtering Quasi-Yagi Antenna based on the high-order mode of SSPPs is fabricated and measured. The final parameters of the proposed high gain wideband filtering quasi-Yagi antenna based on the high-order mode of SSPPs are as follows:  $L=89.9$ mm,  $L_1=4$ mm,  $L_2=19.6$ mm,  $L_3=30.8$ mm,  $L_4=17.2$ mm,  $L_5=15$ mm,  $L_6=10$ mm,  $L_7=9.5$ mm,  $L_8=3$ mm,  $L_{b1}=9$ mm,  $L_{b2}=19.9$ mm,  $L_g=40.6$ mm,  $W=59.3$ mm,  $W_g=46$ mm,  $W_1=2.4$ mm,  $W_2=2$ mm,  $W_3=2$ mm,  $W_4=1.5$ mm,  $W_5=4.6$ mm,  $D_1=20.1$ mm,  $w_0=0.7$ mm,  $w_1=1.6$ mm,  $w_c=1.9$ mm,  $h_c=22$ mm,  $p=11.3$ mm.

The photograph of the proposed High Gain Wideband Filtering Quasi-Yagi Antenna based on the high-order mode of SSPPs is shown in Fig. 15. Considering the practical requirements in communication systems, Fig. 14 illustrates the radiation patterns of the proposed antenna in the E (XOY) and H (YOZ) planes at frequencies of 4 GHz, 5 GHz, 5.2 GHz, 5.8 GHz, and 6 GHz, respectively. The results demonstrate good end-fire characteristics with well-suppressed sidelobes. Across the entire passband, the measured cross-polarization levels in the E-plane and H-plane are below  $-16.4$  dB and  $-15$  dB, respectively. The measured and simulated S-parameters and realized gains are presented in Fig. 16. Measurement results indicate that the reflection coefficient  $|S_{11}|$  is below  $-10$  dB within the range of 3.76 GHz to 6.3 GHz, achieving a fractional bandwidth (FBW) of 50.5%, which closely aligns with the simulation. The measured peak gain within the passband is 9.98 dBi at 5.7 GHz. Additionally, the antenna achieves 18.8 dB out-of-band suppression. To further highlight the advantages of the proposed antenna, a performance comparison with previously reported antennas of similar types in terms of gain, bandwidth, and out-of-band suppression is presented in Table I. It can be observed that the proposed Quasi-Yagi antenna based on the high-order mode of SSPPs features a simple structure, wide bandwidth, excellent out-of-band suppression, and high gain.

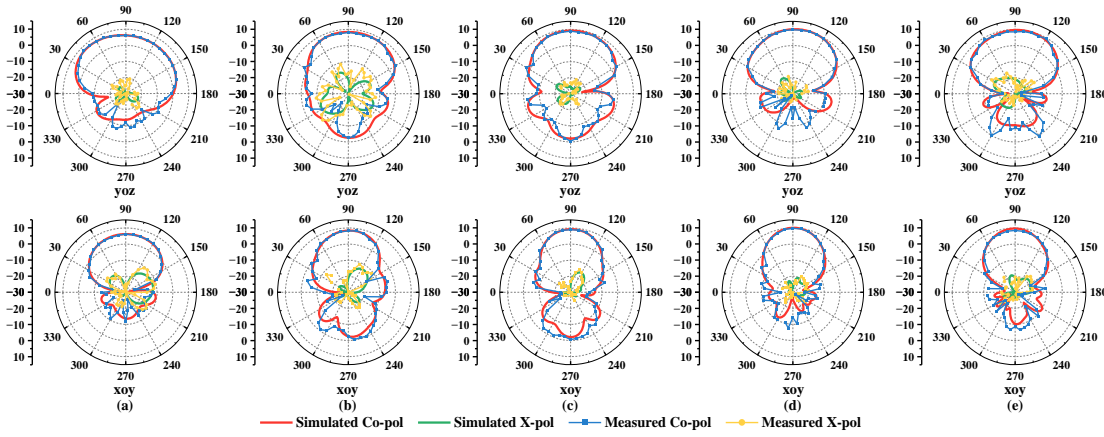


Fig. 14. Measured and simulated radiation patterns of the proposed filtering quasi-Yagi antenna prototype at (a) 4 GHz. (b) 5GHz. (c) 5.2 GHz. (d) 5.8GHz. (e) 6GHz.

TABLE I  
COMPARISON OF THE PROPOSED ANTENNA WITH SOME EXISTING WORKS

Ref.	FBW	P.G. (dBi)	Nulls	Sup. (dB)	R.O.R. (dB/GHz)	Size( $\lambda_0^3$ )	Filtering Design Method
[1]	18.5%	5.8	2	10/15	16/42	$0.76 \times 0.44 \times 0.01$	Stub-loaded resonator
[2]	85.1%	8.3	6	14/17	16/12	$0.49 \times 0.35 \times 0.01$	Exponential curved branch + Parasitic elements
[7]	50%	8.1	3	30/16	51/40	$1.03 \times 1.03 \times 0.24$	Balun feed
[20]	57.1%	10	0	12/12	1.4/12	$2.652 \times 0.980 \times 0.035$	Fundamental mode of SSPPs
[24]	10.44%	9.38	2	26/17	21/72	$4.344 \times 1.529 \times 0.03$	Fundamental mode of SSPPs+ Via holes + Ring resonators
<b>This work</b>	<b>50.5%</b>	<b>9.98</b>	<b>6</b>	<b>21/19</b>	<b>92/58</b>	<b><math>1.507 \times 0.994 \times 0.013</math></b>	<b>High-order Mode of SSPPs</b>

Ref.: Reference, P.G.: Peak Gain, Sup.: Suppression, R.O.R.: Roll-off Rate

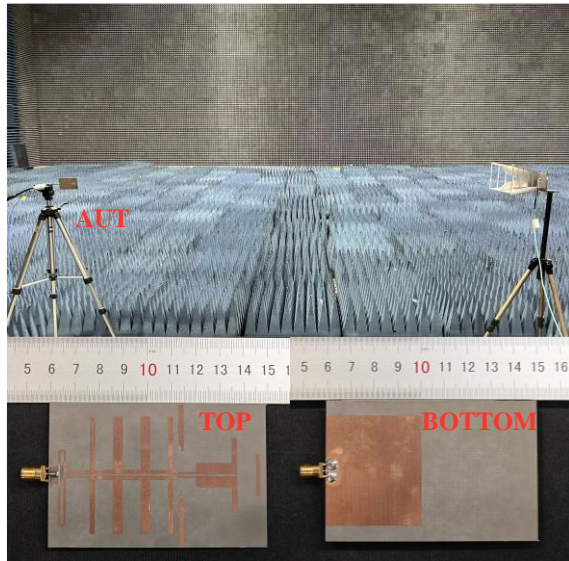


Fig. 15. Photograph of fabricated high gain wideband quasi-Yagi filtering antenna based on high-order mode of SSPPs.

## V. CONCLUSION

In this paper, a high-gain, wideband filtering antenna based on the high-order mode of SSPPs is proposed. By adjusting the

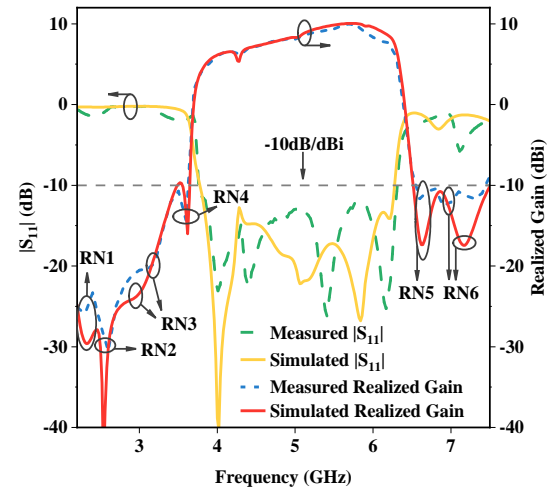


Fig. 16. Measured and simulated results of the proposed high gain wideband filtering quasi-Yagi antenna based on high-order mode of SSPPs.

the geometry of the metallic strips, a feedline operating in the high-order mode of SSPPs with single-mode transmission characteristics is achieved in the target frequency band. Combined with a specially designed balun and ground plane, excellent filtering characteristics with six radiation nulls are obtained. The novel GFSTS, serving as a compact alternative to traditional tapered transitions, facilitates momentum transition

and impedance matching between the SSPPs feedline and the driven dipole, ensuring efficient energy transfer. Leveraging the low-loss characteristics of the SSPPs feedline, this design avoids the insertion loss typical of traditional filtering structures, enhancing radiation efficiency while providing the filtering function of a quasi-Yagi antenna. The measured peak gain reaches 9.98 dBi, with the antenna demonstrating excellent end-fire radiation characteristics. The proposed antenna is fabricated and measured, and the measured and simulated results agree well.

## REFERENCES

[1] F. Wei, X.-B. Zhao, and X. W. Shi, "A Balanced Filtering Quasi-Yagi Antenna With Low Cross-Polarization Levels and High Common-Mode Suppression," *IEEE Access*, vol. 7, pp. 100113–100119, 2019, doi: 10.1109/ACCESS.2019.2931141.

[2] D. Li, C. Yang, Y. Liu, L. Yang, and Q. Chen, "Planar Printed Wideband Filtering Quasi-Yagi Antenna and Its Notch-Band Design Using Parasitic Elements for Vehicular Communication," *IEEE Trans. Veh. Technol.*, vol. 73, no. 2, pp. 2122–2131, Feb. 2024, doi: 10.1109/TVT.2023.3314974.

[3] D. Li, C. Yang, L. Shi, Y. Liu, Q. Chen, and N. Shinohara, "A high gain filtering quasi-yagi antenna based on compressed third-order mode dipole," *IEEE Antennas Wireless Propag. Lett.*, pp. 1–5, 2024, doi: 10.1109/LAWP.2024.3409748.

[4] J. Deng, S. Hou, L. Zhao, and L. Guo, "Wideband-to-narrowband tunable monopole antenna with integrated bandpass filters for UWB/WLAN applications," *IEEE Antennas Wireless Propag. Lett.*, vol. 16, pp. 2734–2737, 2017, doi: 10.1109/LAWP.2017.2743258.

[5] R. Hou, J. Ren, Y.-T. Liu, Y.-M. Cai, J. Wang, and Y. Yin, "Broadband magnetolectric dipole filtering antenna for 5G application," *IEEE Antennas Wireless Propag. Lett.*, vol. 22, no. 3, pp. 497–501, Mar. 2023, doi: 10.1109/LAWP.2022.3216688.

[6] X. Liu, K. W. Leung, and N. Yang, "Frequency reconfigurable filtering dielectric resonator antenna with harmonics suppression," *IEEE Trans. Antennas Propag.*, vol. 69, no. 6, pp. 3224–3233, Jun. 2021, doi: 10.1109/TAP.2020.3044387.

[7] S. J. Yang, Y. F. Cao, Y. M. Pan, Y. Wu, H. Hu, and X. Y. Zhang, "Balun-fed dual-polarized broadband filtering antenna without extra filtering structure," *IEEE Antennas Wireless Propag. Lett.*, vol. 19, no. 4, pp. 656–660, Apr. 2020, doi: 10.1109/LAWP.2020.2975844.

[8] C. F. Ding, X. Y. Zhang, and M. Yu, "Simple dual-polarized filtering antenna with enhanced bandwidth for base station applications," *IEEE Trans. Antennas Propag.*, vol. 68, no. 6, pp. 4354–4361, Jun. 2020, doi: 10.1109/TAP.2020.2975282.

[9] Q. Liu and L. Zhu, "A compact wideband filtering antenna on slots-loaded square patch radiator under triple resonant modes," *IEEE Trans. Antennas Propag.*, vol. 70, no. 10, pp. 9882–9887, Oct. 2022, doi: 10.1109/TAP.2022.3184494.

[10] W. Yang et al., "A simple, compact filtering patch antenna based on mode analysis with wide out-of-band suppression," *IEEE Trans. Antennas Propag.*, vol. 67, no. 10, pp. 6244–6253, Oct. 2019, doi: 10.1109/TAP.2019.2922770.

[11] N.-W. Liu, Y.-D. Liang, L. Zhu, Z.-X. Liu, and G. Fu, "A low-profile, wideband, filtering-response, omnidirectional dielectric resonator antenna without enlarged size and extra feeding circuit," *IEEE Antennas Wireless Propag. Lett.*, vol. 20, no. 7, pp. 1120–1124, Jul. 2021, doi: 10.1109/LAWP.2021.3072062.

[12] W. Yang, M. Xun, W. Che, W. Feng, Y. Zhang, and Q. Xue, "Novel compact high-gain differential-fed dual-polarized filtering patch antenna," *IEEE Trans. Antennas Propag.*, vol. 67, no. 12, pp. 7261–7271, Dec. 2019, doi: 10.1109/TAP.2019.2930213.

[13] J.-Y. Lin, Y. Yang, S.-W. Wong, and Y. Li, "High-order modes analysis and its applications to dual-band dual-polarized filtering cavity slot arrays," *IEEE Trans. Microw. Theory Techn.*, vol. 69, no. 6, pp. 3084–3092, Jun. 2021, doi: 10.1109/TMTT.2021.3072945.

[14] R. Lu et al., "SIW cavity-fed filtennas for 5G millimeter-wave applications," *IEEE Trans. Antennas Propag.*, vol. 69, no. 9, pp. 5269–5277, Sep. 2021, doi: 10.1109/TAP.2021.3061110.

[15] J.-F. Qian, F.-C. Chen, Y.-H. Ding, H.-T. Hu, and Q.-X. Chu, "A wide stopband filtering patch antenna and its application in MIMO system,"

*IEEE Trans. Antennas Propag.*, vol. 67, no. 1, pp. 654–658, Jan. 2019, doi: 10.1109/TAP.2018.2874764.

[16] X. Gao et al., "Ultra-wideband surface plasmonic Y-splitter," *Opt. Express*, vol. 23, no. 18, pp. 23270–23277, Sep. 2015, doi: 10.1364/OE.23.023270.

[17] Q. L. Zhang and C. H. Chan, "Compact Spoof Surface Plasmon Polaritons Waveguide Integrated With Blind Vias and Its Applications," *IEEE Trans. Circuits Syst. II*, vol. 67, no. 12, pp. 3038–3042, Dec. 2020, doi: 10.1109/TCSII.2020.3001297.

[18] C. H. Wang, X. M. Shi, H. L. Yang, and X. L. Xi, "A Flexible Amplitude Equalizing Filter Based on Spoof Surface Plasmon Polaritons," *IEEE Trans. Antennas Propag.*, vol. 71, no. 7, pp. 5777–5785, Jul. 2023, doi: 10.1109/TAP.2023.3266864.

[19] X. Du, H. Li, and Y. Yin, "Wideband fish-bone antenna utilizing odd-mode spoof surface plasmon polaritons for endfire radiation," *IEEE Trans. Antennas Propag.*, vol. 67, no. 7, pp. 4848–4853, Jul. 2019, doi: 10.1109/TAP.2019.2913707.

[20] Huanhuan Qi and Haiwen Liu, "Wideband High-Gain Filtering Vivaldi Antenna Design Based on MS and Herringbone SSPP Structure," *IEEE Antennas Wireless Propag. Lett.*, vol. 22, no. 8, pp. 1798–1802, Aug. 2023, doi: 10.1109/LAWP.2023.3264702.

[21] Z. Lin, Y. Li, L. Li, Y.-T. Zhao, J. Xu, and J. Chen, "Miniaturized bandpass filter based on high-order mode of spoof surface plasmon polaritons loaded with capacitor," *IEEE Trans. Plasma Sci.*, vol. 51, no. 1, pp. 254–260, Jan. 2023, doi: 10.1109/TPS.2022.3232850.

[22] K.-D. Xu, S. Lu, Y.-J. Guo, and Q. Chen, "High-Order Mode of Spoof Surface Plasmon Polaritons and Its Application in Bandpass Filters," *IEEE Trans. Plasma Sci.*, vol. 49, no. 1, pp. 269–275, Jan. 2021, doi: 10.1109/TPS.2020.3043889.

[23] Z. Liang, S.-S. Qi, and W. Wu, "Ultra-Wideband Planar End-Fire Antenna Based on High-Order Modes of Spoof Surface Plasmon Polaritons," *IEEE Trans. Antennas Propag.*, vol. 71, no. 2, pp. 1469–1477, Feb. 2023, doi: 10.1109/TAP.2022.3227750.

[24] Wenjie Feng, Yanhao Feng, Wanchen Yang, Wenquan Che, and Quan Xue, "High-performance filtering antenna using spoof surface plasmon polaritons," *IEEE Trans. Plasma Sci.*, vol. 47, no. 6, pp. 2832–2837, Jun. 2019, doi: 10.1109/TPS.2019.2915627.

[25] A. Kandwal, Q. Zhang, X.-L. Tang, L. W. Liu, and G. Zhang, "Low-profile spoof surface plasmon polaritons traveling-wave antenna for near-endfire radiation," *IEEE Antennas Wireless Propag. Lett.*, vol. 17, no. 2, pp. 184–187, Feb. 2018, doi: 10.1109/LAWP.2017.2779455.



**Daotong Li** (Senior Member, IEEE) received the Ph.D. degree in electromagnetic field and microwave technology from the University of Electronic Science and Technology of China, Chengdu, China, in 2016. He is currently with the Center of Tracking Telemetry Command, Chongqing University, Chongqing.

He has been a Visiting Researcher with the Department of Electrical and Computer Engineering, University of Illinois at Urbana-Champaign from 2015 to 2016, later joining Chongqing University as Assistant Professor in 2017 and being promoted to Associate Professor in 2019. His academic journey includes being awarded a JSPS Fellowship at Tohoku University from Nov.2021 to Nov. 2023, and serving as a visiting associate professor at Kyoto University in 2024, and being a Guest Scholar since June 2024. His research focuses on RF/microwave/millimeter-wave technologies, microwave power transmission (MPT), and antennas, with over 100 peer-reviewed publications. His achievements include receiving the UESTC Outstanding Graduate Awards (2016), National Graduate Student Scholarship, and "Tang Lixin" Scholarship. His professional service includes reviewing for IEEE/IET journals and participating in international conferences as TPC Member, Session Organizer and Chair.



**Ning Pan** received the B.S. degree in Yantai University, China, in 2023. He is currently pursuing the M.S. degree in Information and Communication Engineering with the School of Microelectronics and Communication Engineering, Chongqing University, China. His current research interests include

polaritons (SPP) devices, and filters.



**Hao Wang** received the B.S. degree in South-Central Minzu University, China, in 2023. He is currently pursuing the M.S. degree in Electronic Information with the School of Microelectronics and Communication Engineering, Chongqing University, China.

His current research interests include microwave circuits and systems.



**Jiang Dong** received the B.S. degree in Chengdu University of Technology, China, in 2022. He is currently pursuing the M.S. degree in Information and Communication Engineering with the School of Microelectronics and Communication Engineering, Chongqing University, China. His current research interests include

microwave power transmission, slot antenna, and array antenna.



**Qi Jiang** received the B.S. degree in Henan University, China, in 2023. He is currently pursuing the M.S. degree in Information and Communication Engineering with the School of Microelectronics and Communication Engineering, Chongqing University, China.

His current research interests include filters, nonreciprocity, and substrate integrated

waveguide devices.



**Ying Liu** received the M.S. degree in communication and information system from the Chongqing University, Chongqing, China, in 2015. She is currently with the College of Microelectronics and Communication Engineering, Chongqing University, Chongqing. Her research focuses on microwave photonics and image

processing.



**Naoki Shinohara** (Fellow, IEEE) received the Ph.D. degree in electrical engineering from the Kyoto University, Kyoto, Japan, in 1996. He is currently a Professor with the Research Institute for Sustainable Humanosphere, Kyoto University, Kyoto. He has been affiliated with Kyoto University since 1996, becoming a

Professor in 2010, where he conducts pioneering research on solar power satellites and microwave power transmission systems. He has authored seminal works including *Wireless Power Transfer via Radiowaves* (Wiley, 2014) and edited several authoritative volumes on wireless power technologies. An IEEE Distinguished Microwave Lecturer (2016-2018) and current IEEE AdCom Member (2022-2024), Dr. Shinohara plays multiple leadership roles across prestigious organizations: he founded the IEEE Wireless Power Transfer Conference and serves on its Steering Committee, chairs URSI Commission D and the Wireless Power Transfer Consortium for Practical Applications (WiPoT), acts as Executive Editor for the *International Journal of Wireless Power Transfer*, and holds vice-chairmanship of the Space Solar Power Systems Society. His extensive committee engagements span IEEE MTT-S Technical Committee 25, IEICE Wireless Power Transfer, and various Japanese research consortia, cementing his status as a global leader in advancing wireless power technologies.



**Qiang Chen** received the B.E. degree from Xidian University, Xi'an, China, in 1986, the M.E. and D.E. degrees from Tohoku University, Sendai, Japan, in 1991 and 1994, respectively. He is currently Chair Professor of Electromagnetic Engineering Laboratory with the Department of Communications Engineering, Faculty of

Engineering, Tohoku University. His primary research interests include antennas, microwave and millimeter wave, electromagnetic measurement, and computational electromagnetics.

He received the Best Paper Award and Zen-ichi Kiyasu Award from the Institute of Electronics, Information and Communication Engineers (IEICE). He served as the Chair of IEICE Technical Committee on Photonics-applied Electromagnetic Measurement from 2012 to 2014, the Chair of IEICE Technical Committee on Wireless Power Transfer from 2016 to 2018, the Chair of IEEE Antennas and Propagation Society Tokyo Chapter from 2017 to 2018, the Chair of IEICE Technical Committee on Antennas and Propagation from 2019 to 2021. IEICE Fellow.